

Probabilistic assessment of response spectra for multiple damping levels in seismic hazard analysis

Haizhong Zhang^a, Rui Zhang^{b,*}, Yan-Gang Zhao^c, Hongjun Si^d, Haixiu Zhang^e

^a Eco-Science Course, Faculty of Agriculture, Yamagata University, 1-23, Wakaba-machi, Tsuruoka-shi, Yamagata, 997-8555, Japan

^b School of Geography and Tourism, Qilu Normal University, Jinan, 250200, China

^c Faculty of Architecture, Civil and Transportation Engineering, Beijing University of Technology, Beijing, 100124, China

^d Seismological Research Institute Inc., Tokyo, Japan

^e Luanping County Branch of Chengde Ecological Environment Bureau, Chengde, China

ARTICLE INFO

Keywords:

Response spectra for multiple damping levels

Probabilistic seismic hazard analysis

Fourier amplitude spectrum

Moment method

Latin hypercube sampling

ABSTRACT

The response spectra for specific recurrence periods are typically constructed for a 5 % damping ratio based on probabilistic seismic hazard analysis (PSHA). Nevertheless, practical structures exhibit a range of damping characteristics, requiring response spectra at various damping levels. Commonly, a damping modification factor (DMF) is applied to adjust the 5 %-damped spectra derived from PSHA to other damping levels. Most DMF formulations, however, are developed solely through the regression analysis of seismic records, overlooking the consistency of the recurrence period of the response spectra before and after adjustment. A direct probabilistic analysis of the response spectra across different damping ratios provides a more reasonable solution, although it typically needs multiple ground motion prediction equations (GMPEs) for each damping level or, alternatively, the application of a DMF to adjust the 5 %-damped GMPE. However, many recent studies have highlighted the difficulty of directly constraining the scaling of the response spectra within GMPEs via seismological theory. To address this issue, this study proposes a new framework for conducting a probabilistic analysis of the response spectra across multiple damping ratios. The framework estimates site-specific response spectra for various damping ratios using a single GMPE for the Fourier amplitude spectrum (FAS) combined with a ground-motion duration model. Because the FAS is more closely related to the physics of wave propagation, its scaling within GMPEs is easier to constrain using seismological theory. Furthermore, the moment method, in conjunction with Latin hypercube sampling, is applied to calculate the exceedance probability for response spectra with any damping ratio, thereby obtaining the corresponding seismic hazard curves. The proposed framework was verified and compared with traditional approaches using a numerical example. The proposed framework enables the acquisition of response spectra for distinct recurrence periods at any desired damping ratio while eliminating the need to construct multiple GMPEs for various damping ratios or to develop DMF models.

1. Introduction

Response spectra corresponding to certain recurrence periods are often utilized to determine seismic forces for structural seismic designs. Commonly, response spectra for specific recurrence periods are constructed for a single 5 % damping ratio based on probabilistic seismic hazard analysis (PSHA) [1–3]. For example, the United States Geological Survey constructed response spectra for 475- and 2475-year recurrence periods based on a 5 % damping ratio, which were then applied to the National-Earthquake-Hazard-Reduction-Program provisions (e.g., the Building Seismic Safety Council, 2015 and 2020) [4,5]. However, in

practice, the damping ratio of structures can vary depending on the materials used and the presence of energy-dissipation systems [6,7]. Therefore, response spectra for the given recurrence periods are necessary not only for the 5 % damping ratio, but also for various other damping ratios to ensure a comprehensive structural design.

Traditionally, to construct the response spectra across various damping ratios, a damping modification factor (DMF) is applied to adjust the 5 %-damped response spectra obtained from PSHA. The DMF, defined as the ratio of the response spectrum at a given damping level to the response spectrum at a damping level of 5 %, has been extensively studied and formulated based on the regression analysis of numerous

* Corresponding author.

E-mail address: zhangrui@qlnu.edu.cn (R. Zhang).

<https://doi.org/10.1016/j.soildyn.2025.109460>

Received 11 January 2025; Received in revised form 15 April 2025; Accepted 16 April 2025

Available online 30 April 2025

0267-7261/© 2025 Published by Elsevier Ltd.

real seismic records [8–13]. Additionally, the DMF has been found to depend on the damping ratio and on various other factors, such as the period, magnitude, distance, and site conditions [8–13]. However, the response spectra of specific seismic records differ from those corresponding to certain recurrence periods that are derived through PSHA by considering various potential earthquake sources and associated uncertainties. The development of the DMF formulations based on specific seismic records cannot consider the recurrence period of response spectra. Therefore, the traditional approach of using the DMF to adjust the response spectra derived from PSHA cannot guarantee the consistency of the recurrence period of the response spectra before and after modification.

To address this issue, a direct probabilistic analysis of response spectra across different damping ratios within the PSHA framework offers a more reasonable solution. This approach typically requires multiple ground motion prediction equations (GMPEs) for each damping level or, alternatively, the application of a DMF to adjust the 5 %-damped GMPE. Some studies, such as that of Akkar and Bommer [14], have developed GMPEs for response spectra at several damping levels in some regions. Additionally, some studies, such as that of Rezaeian et al. [15], have developed DMFs to adjust the 5 %-damped GMPEs of the response spectra to other damping levels. Nevertheless, recent studies have highlighted the difficulty associated with the direct constraint of the scaling of response spectra within GMPEs via seismological theory [16–19]. This difficulty arises because response spectral scaling is dependent on the spectral shape, causing the linear source, path, and site effects to scale differently on the spectral values between small and large magnitudes [20,21].

To address the above challenges, this study proposes a new framework for conducting a probabilistic analysis of response spectra with various damping ratios. This framework adopts the GMPE for the Fourier amplitude spectrum (FAS) coupled with a ground-motion duration model. Because Fourier spectra are more closely related to the physics of wave propagation, the scaling of the FAS in GMPEs is more easily constrained via seismological theory than is the scaling of response spectra [20,21]. Subsequently, the response spectra for different damping ratios are estimated from the FAS and duration based on random vibration theory (RVT), eliminating the need for multiple GMPEs for response spectra or DMF adjustments. Moreover, the moment method, in conjunction with Latin hypercube sampling (LHS), is applied to calculate the exceedance probability for response spectra with any damping ratio, thereby obtaining the corresponding seismic hazard curves. The remainder of this paper is organized as follows. Section 2 describes traditional approaches for generating response spectra for specific recurrence periods across various damping ratios. Section 3 presents the method for estimating response spectra for different damping ratios from the FAS and duration based on RVT. Section 4 shows the approach for calculating the exceedance probability for response spectra for any damping ratio and obtaining the corresponding seismic hazard curves. Section 5 validates the proposed framework and compares it with traditional approaches using a numerical example. Section 6 concludes the paper with a summary of the findings.

2. Traditional approaches for generating response spectra for specific recurrence periods across various damping ratios

This section briefly reviews traditional approaches for generating response spectra for specific recurrence periods across various damping ratios. Commonly, the pseudo spectral acceleration (PSA) for specific recurrence periods is constructed for a 5 % damping ratio based on PSHA. For this purpose, all earthquake faults/zones capable of producing damaging ground motions need to be identified, and their recurrence, magnitude, and distance distributions should be evaluated. Then, the GMPEs for the 5 %-damped PSA are selected to estimate the ground motion intensity at the sites of interest. Finally, the exceedance probabilities for the 5 %-damped PSA and the corresponding seismic hazard

curves are calculated considering all earthquake faults/zones. Specifically, the probability that the PSA exceeds a specified value psa during a specified period t (years), $P(\text{PSA} > psa, t)$, can be estimated using the following equation:

$$P(\text{PSA} > psa, t) = 1 - \prod_{k=1}^m [1 - P_k(\text{PSA} > psa, t)] \quad (1)$$

where k refers to the k th earthquake fault/zone, m represents the number of earthquake faults/zones capable of producing damaging ground motions, and $P_k(\text{PSA} > psa, t)$ is the exceedance probability calculated by considering only the k th earthquake fault/zone. If the occurrence of seismic events follows a homogeneous stochastic Poisson process, $P_k(\text{PSA} > psa, t)$ can be expressed as

$$P_k(\text{PSA} > psa, t) = 1 - e^{-p_k \nu_k t} \quad (2)$$

Here, ν_k is the mean annual rate of the k th earthquake fault/zone, and p_k is the exceedance probability of the k th earthquake given the occurrence of the earthquake, which is expressed as

$$p_k(\text{PSA} > psa) = \int_R \int_M P(\text{PSA} > psa, |m, r) f_M(m) f_R(r) dm dr \quad (3)$$

where $f_M(m)$ represents the probability density function (PDF) of the magnitude occurring in the source and $f_R(r)$ is the PDF used to describe the randomness of the epicenter locations within the source. Additionally, $P(\text{PSA} > psa |m, r)$ is the probability that the PSA exceeds a specified value psa given a magnitude m and distance r . $P(\text{PSA} > psa |m, r)$ is commonly estimated using a GMPE for the 5 %-damped PSA assuming that the natural logarithm of the PSA for a given magnitude and distance follows a normal distribution.

After the PSA for a 5 % damping ratio corresponding to the specific recurrence periods is obtained using Eqs. (1)–(3), the PSA for other damping ratios can be derived using a DMF to adjust the 5 %-damped PSA, which can be expressed as

$$\text{PSA}(\xi) = \text{DMF}(\xi) \times \text{PSA}(5\%) \quad (4)$$

where $\text{PSA}(\xi)$ represents the PSA for a damping ratio ξ , $\text{DMF}(\xi)$ is the DMF corresponding to ξ , and $\text{PSA}(5\%)$ represents the PSA for a damping ratio of 5 %. Commonly, the DMF, defined as the ratio of the PSA at a given damping level to the PSA at 5 % damping, is derived based on real seismic records [8–13]. However, the PSA values obtained from specific seismic records differ from those associated with particular recurrence periods, which are derived through PSHA by accounting for various potential earthquake sources and uncertainties. The development of DMF formulations based on specific seismic records does not consider the recurrence periods of the PSA. As a result, the conventional method of applying a DMF to adjust the PSA derived from PSHA cannot ensure the consistency of the recurrence period of the PSA before and after modification.

A more reasonable approach to generating the PSA for specific recurrence periods across various damping ratios is to directly conduct a probabilistic analysis of the PSA across different damping ratios within the PSHA framework. This approach simply requires replacing the 5 %-damped PSA GMPE in the calculation of $P(\text{PSA} > psa |m, r)$ using Eq. (3) within the traditional PSHA framework with GMPEs corresponding to the desired damping ratios. Obviously, this approach needs multiple GMPEs for each damping level or the application of a DMF to adjust the 5 %-damped GMPE. However, many recent studies have highlighted the challenge associated with directly constraining the scaling of the PSA within GMPEs via seismological theory [16–19]. This challenge arises because the response spectral scaling is dependent on the spectral shape, implying that the linear source, path, and site effects do not scale uniformly on the spectral values for small and large magnitudes [20,21].

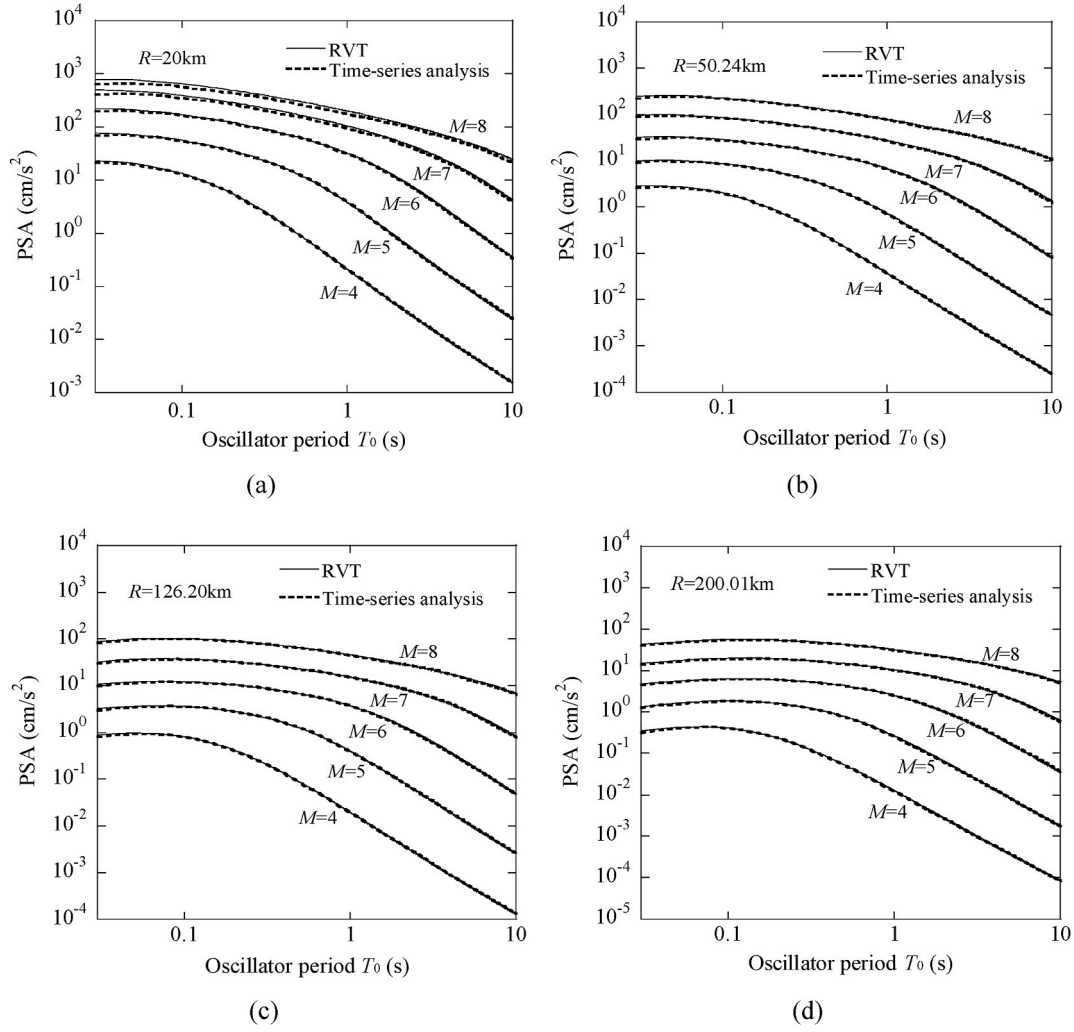


Fig. 1. Comparisons of PSA results for a 10 % damping ratio calculated using Eq. (5) and time-series analysis for (a) $R = 20$ km, (b) $R = 50.24$ km, (c) $R = 126.20$ km, and (d) $R = 200.01$ km.

3. Estimation of response spectra at different damping ratios

To address the aforementioned issue, it is preferable to avoid using multiple GMPEs for PSA or DMF adjustments. Boore [22] proposed a method capable of estimating the PSA for any damping ratio by combining the FAS with the duration of ground motion based on RVT. Hence, by using a single GMPE for the FAS along with a duration model, the PSA for any damping ratio can be easily derived. In addition, since Fourier spectra are closely related to the physics of wave propagation, the scaling of the FAS in GMPEs is more easily constrained via seismological theory than the scaling of PSA [16–19]. In recent years, many studies have preferred to use the GMPE for the FAS and developed many FAS GMPEs [16,20,21,23]. Therefore, this study adopts the FAS GMPE coupled with a ground-motion duration model to estimate the PSA for various damping ratios.

3.1. PSA for various damping ratios

Boore [22] derived an equation capable of estimating the PSA for any damping ratio using the FAS and duration of ground motion based on RVT, which is expressed as

$$PSA(\omega, \xi) = pf \sqrt{\frac{1}{D_{rms}\pi} \int_0^\infty |Y(\omega) \times I(\omega, \xi)|^2 d\omega} \quad (5)$$

where $Y(\omega)$ is the acceleration FAS of the ground motion, ω is the circular frequency of the ground motion, pf represents the peak factor, and D_{rms} denotes the root-mean-square (RMS) duration of the single-degree-of-freedom (SDOF) oscillator response (details presented subsequently). In addition, the square-root term in Eq. (5) represents the RMS value of the oscillator response. $Y(\omega) \times I(\omega, \xi)$ denotes the oscillator-response FAS, whereas $I(\omega, \xi)$ represents the oscillator transfer function, which is expressed as follows:

$$I(\omega, \xi) = \frac{1}{\sqrt{(2\xi\omega/\bar{\omega})^2 + ((\omega/\bar{\omega})^2 - 1)^2}} \quad (6)$$

where $\bar{\omega}$ and ξ are the circular frequency and damping ratio of the SDOF oscillator, respectively.

In Eq. (5), pf represents the peak factor. Many peak-factor models have been developed for RVT analyses [24–26]. Although the Cartwright and Longuet-Higgins model [24] has been commonly applied in engineering seismology and site response analyses, the Vanmarcke model [26] can give better estimations of the peak factor [27]. The cumulative distribution function (CDF) of the peak factor pf provided by the Vanmarcke model [26] is expressed as follows:

$$P(pf < r) = [1 - e^{-(r^2/2)}] \times \exp \left[-2f_z e^{-(r^2/2)} D_{gm} \frac{(1 - e^{\delta^{1/2} r \sqrt{\pi/2}})}{(1 - e^{r^2/2})} \right] \quad (7)$$

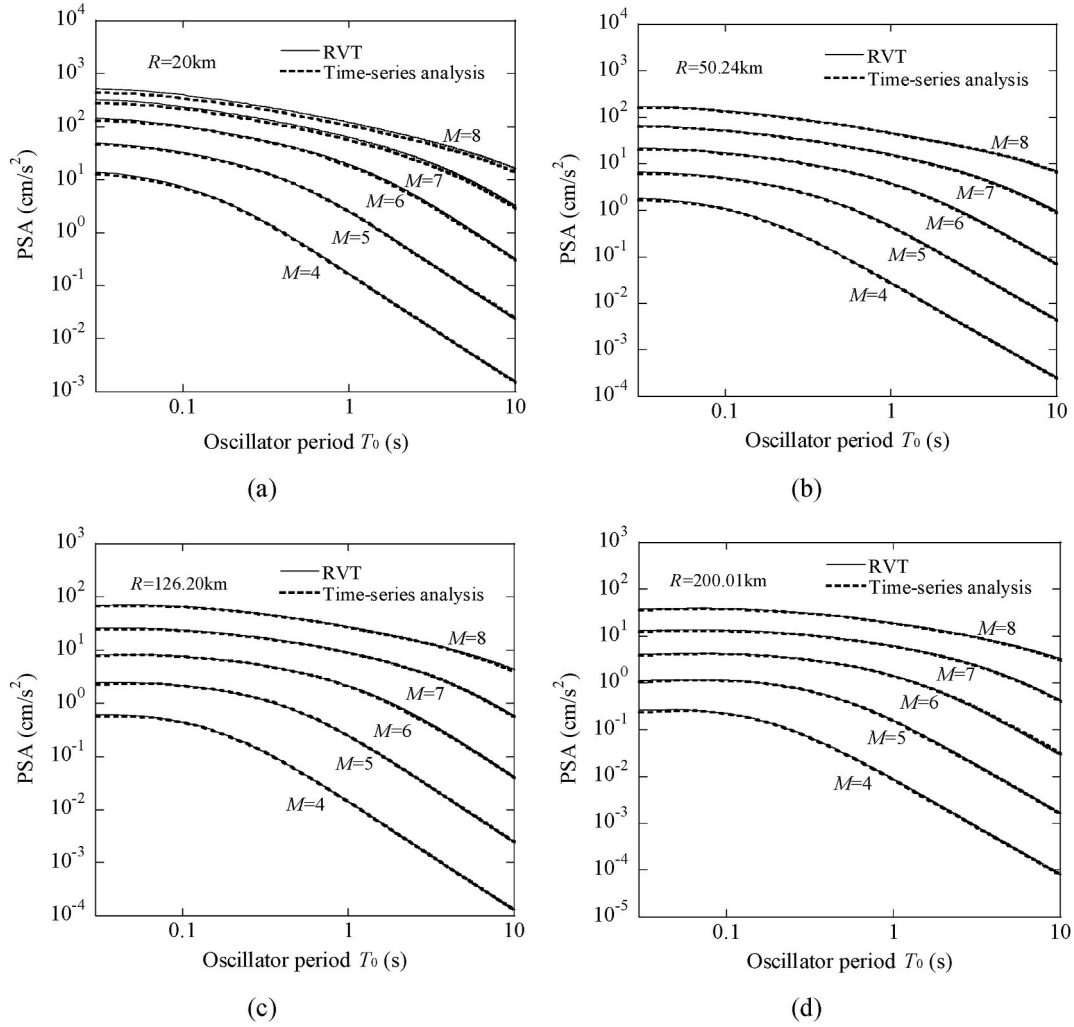


Fig. 2. Comparisons of PSA results for a 30 % damping ratio calculated using Eq. (5) and time-series analysis for (a) $R = 20$ km, (b) $R = 50.24$ km, (c) $R = 126.20$ km, and (d) $R = 200.01$ km.

Here, D_{gm} represents the ground-motion duration, and δ is a bandwidth factor defined as a function of the spectral moments:

$$\delta = \sqrt{1 - \frac{m_1^2}{m_0 m_2}} \quad (8)$$

where m_0 , m_1 , and m_2 denote the zeroth-, first-, and second-order moments of the square of the FAS, respectively. The n th-order spectral moment, m_n , can be expressed as,

$$m_n = \frac{1}{\pi} \int_0^\infty \omega^n (Y(\omega) \times I(\omega, \xi))^2 d\omega \quad (9)$$

In addition, f_z denotes the rate of zero crossings, which is also a function of the spectral moments and is given by

$$f_z = \frac{1}{2\pi} \sqrt{\frac{m_2}{m_0}} \quad (10)$$

In RVT analyses, the expected value of pf is typically used. According to Eq. (7), the expected value of pf can be calculated as $\int_0^\infty [1 - P(pf < r)] dr$.

For the estimation of the PSA using Eq. (5) based on RVT, some basic assumptions, such as the quasi-stationarity of the equivalent time series and the statistical independence of the consecutive maxima of the time series [28–30], are made. These assumptions are not inherently satisfied

by seismic ground motions, leading to discrepancies between RVT and time-series analyses. To overcome these limitations, the RMS duration of the oscillator response D_{rms} was proposed to correct the errors in the PSA arising from these assumptions [28–30]. Boore and Joyner [28] and Liu and Pezeshk [29] developed simple formulas to calculate the RMS duration D_{rms} from D_{gm} . Boore and Thompson [30] then developed a more accurate formula for D_{rms} as

$$\frac{D_{rms}}{D_{gm}} = \left(c_{e1} + c_{e2} \frac{1 - \eta^{c_{e3}}}{1 + \eta^{c_{e3}}} \right) \left[1 + \frac{c_{e4}}{2\pi\xi} \left(\frac{\eta}{1 + c_{e5}\eta^{c_{e6}}} \right)^{c_{e7}} \right] \quad (11)$$

Here, $\eta = T_0/D_{gm}$, T_0 is the SDOF oscillator period, and c_{e1} – c_{e7} are coefficients that depend on the moment magnitude M and site-to-source distance R , as noted by Boore and Thompson [30].

3.2. Comparison with time-series analysis

Equation (5) has been widely employed to estimate the PSA for a 5 % damping ratio, and its effectiveness in this regard has been well verified [22,27,30]. Although Zhang and Zhao [10,31] applied Eq. (5) in estimating the PSA for various damping ratios, the accuracy of this application has not yet been comprehensively and directly verified. To demonstrate the accuracy of Eq. (5) in estimating the PSA for various damping ratios, the PSA values for damping ratios of 10 %, 20 %, 30 %, 40 %, and 50 % were calculated using Eq. (5). Subsequently, these results were compared with those obtained from traditional time-series

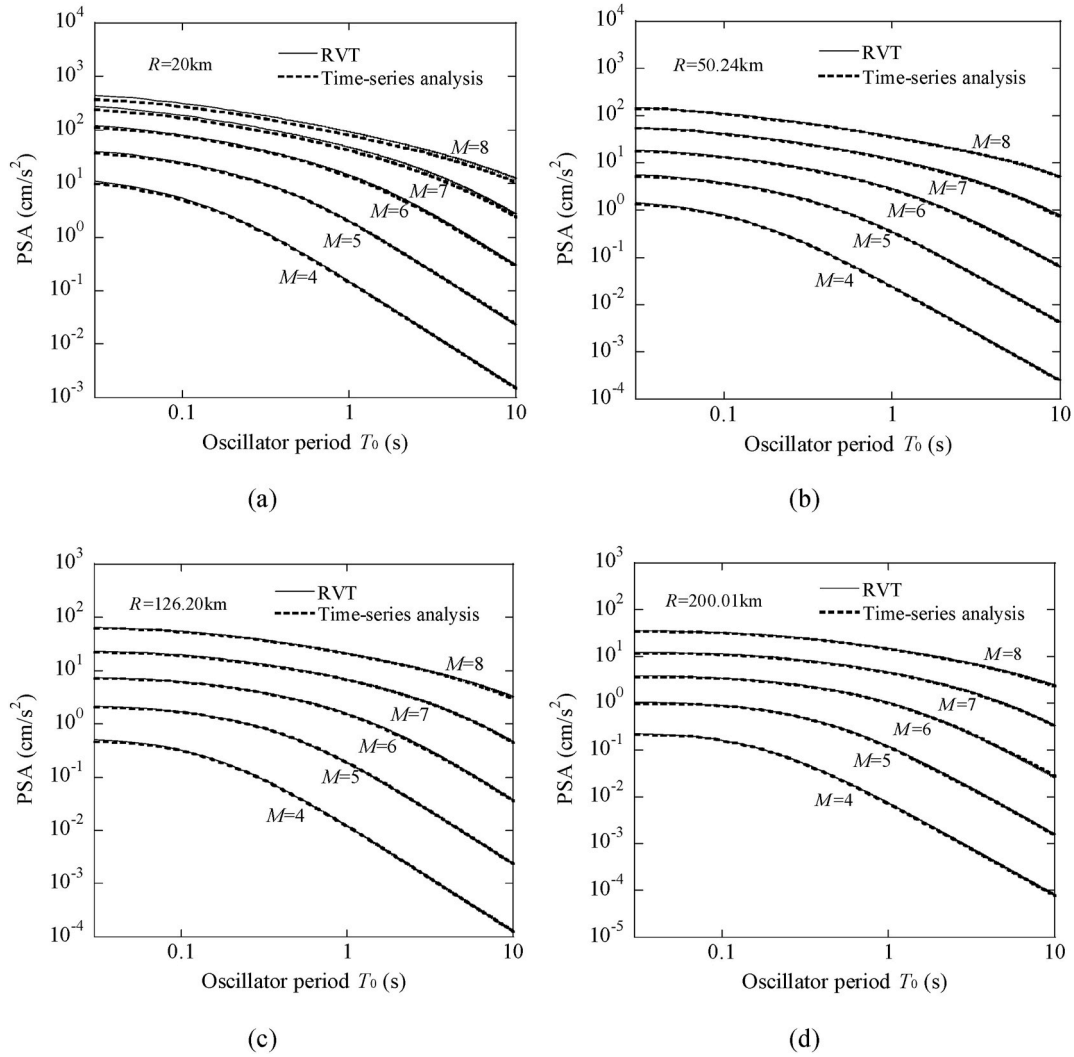


Fig. 3. Comparisons of PSA results for a 50 % damping ratio calculated using Eq. (5) and time-series analysis for (a) $R = 20$ km, (b) $R = 50.24$ km, (c) $R = 126.20$ km, and (d) $R = 200.01$ km.

analysis. The FAS $Y(\omega)$ was generated based on a widely used point-source FAS model introduced by Boore [22]. The values of the seismological parameters required for this model were determined according to Boore and Thompson [30] and are consistent with those used by Zhang et al. [32]. The time series for the analysis were generated from the FAS using the stochastic method simulation program [33,34]. For each FAS, a suite of 100 time series signals were generated, and the average FAS of the simulated time series matched the target FAS. A wide range of oscillator periods T_0 (0.02–10 s), moment magnitudes M (4–8), and site-to-source distances R (20–200.01 km) were considered in the calculations.

The PSA values for the generated time series were calculated using the direct-integration method proposed by Nigam and Jennings [35]. For each FAS, the 100 corresponding PSA results were averaged and compared with those obtained using Eq. (5). Some of these comparisons are shown in Figs. 1–3. Figs. 1–3 show the PSA results for 10 %, 30 %, and 50 % damping, respectively. The favorable agreement shown in these figures confirms the accuracy of the estimated PSA values at different damping ratios using Eq. (5). In addition, the accuracy of RVT remains nearly unchanged for different damping ratios, even when the damping ratio is increased to 50 %. This suggests that although the D_{rms} formula was originally proposed to correct errors in the PSA arising from the basic assumptions of RVT for a single 5 % damping ratio [30], it is also applicable to other damping ratios.

4. Seismic hazard curves of response spectra with different damping ratios

It is evident from Eq. (3) that the calculation of exceedance probabilities or seismic hazard curves requires solving multiple integrals that are generally difficult to handle theoretically. It is common practice in the traditional PSHA framework to discretize the continuous distributions of M and R and convert the integrals into discrete summations [36]. Each element within these discrete summations can be treated as an individual earthquake characterized by magnitude, distance, and focal parameters, etc. Because the natural logarithm of the PSA for a given magnitude and distance is typically considered to follow a normal distribution, the probability that the PSA exceeds a specified value P ($PSA > p_{sa}/m, r$) can be directly obtained using the CDF of the normal distribution. Ultimately, the exceedance probability $p_k(PSA > p_{sa})$ can be obtained by summing that of each discrete earthquake.

However, employing such an approach to compute the exceedance probability $p_k(PSA > p_{sa})$ within the proposed framework is not feasible. This is due not only to the additional integrals required to compute the PSA for various damping ratios from the FAS (Eqs. (5)–(11)) but also, more importantly, to the unfeasibility of estimating $P(PSA > p_{sa}/m, r)$ directly from a given PDF of the FAS. This difficulty arises because the proposed framework relies on the GMPE for the FAS and ground-motion duration model, instead of directly using GMPEs for

the PSA. Consequently, although the PDF for the FAS is provided in its GMPE, the PDF for the PSA remains unknown. To address these challenges, Monte Carlo (MC) simulation can be used. Specifically, (1) generate enough samples for each random variable following the given distributions; (2) estimate the PSA results for various damping ratios according to the generated samples for each random variable using Eq. (5); and (3) calculate the exceedance probability $p_k(\text{PSA} > \text{psa})$ by statistical analysis of all the obtained results. The accuracy of the MC simulation results depends on the number of generated samples for each random variable, it increases with increasing sample number. We attempted to calculate $p_k(\text{PSA} > \text{psa})$ using 100000 samples for each random variable, which is considered the number necessary to obtain reliable results corresponding to a usually used return period of 500 years. However, this takes approximately 30 min for a single oscillator period and a single damping ratio considering one source. If multiple sources, oscillator periods, and damping ratios are considered in real cases, MC simulation becomes impractical.

Therefore, to simplify the calculation, an efficient method, namely the moment method [37], is adopted in this study. The moment method calculates the exceedance probability $p_k(\text{PSA} > \text{psa})$ using two fundamental steps: (1) a distribution form is assumed for the PSA defined in terms of the first several statistical moments, and (2) the first several statistical moments are estimated according to the PDFs of the basic random variables including M , R , and the residuals in the GMPE for the FAS and ground-motion duration model.

The natural logarithm of the PSA is assumed to follow a three-parameter distribution defined in terms of the mean value, deviation, and skewness [38,39]. The three-parameter distribution was selected because it can better fit statistical data, particularly those associated with skewness, than traditional two-parameter distributions, e.g., normal and lognormal distributions. This is discussed in detail in the next section. The CDF of the three-parameter distribution corresponding to $p_k(\ln(\text{PSA}) > \ln(\text{psa}))$ is expressed as

$$F_k(\ln(\text{PSA})) = \Phi \left[\frac{1}{\alpha_3} \left(\sqrt{9 + \frac{1}{2}\alpha_3^2 + 6\alpha_3 \frac{\ln(\text{PSA}) - \mu_1}{\sigma_{\text{PSA}}}} \cdot \sqrt{9 - \frac{1}{2}\alpha_3^2} \right) \right] \quad (12)$$

where μ_1 , σ_{PSA} , and α_3 are the mean value, standard deviation, and skewness of $\ln(\text{PSA})$, respectively. The standard deviation σ_{PSA} and the skewness α_3 can be estimated using the following equations:

$$\sigma_{\text{PSA}} = \sqrt{\mu_2 - \mu_1^2} \quad (13)$$

$$\alpha_3 = \frac{\mu_3 - 3\mu_2\mu_1 + 2\mu_1^3}{\sigma_{\text{PSA}}^3} \quad (14)$$

where μ_1 , μ_2 , and μ_3 are the first-, second-, and three-order statistical moments of $\ln(\text{PSA})$, respectively. Note that once the three statistical moments are determined, $F_k(\ln(\text{PSA}))$ and the seismic hazard curves can be obtained. In theory, the k th-order statistical moment μ_k is expressed as,

$$\mu_k = E[(\ln(\text{PSA}))^k] = \int \int \int \int (\ln(\text{PSA}))^k f_M(m) f_R(r) f_{R_{\text{FAS}}}(r_{\text{FAS}}) f_{R_D}(r_D) dm dr_{\text{FAS}} dr_D \quad (15)$$

where R_{FAS} represents the residual in the GMPE for the FAS and R_D represents the residual in the ground-motion duration D_{gm} model.

It can be noted that Eq. (15) also contains complex multiple integrals. To simplify the calculation, the LHS simulation was adopted to calculate the first three statistical moments [40]. Unlike MC simulation, which relies on random sampling, LHS uses a stratified sampling strategy. This approach ensures that each segment of the input range is sampled, thereby providing more comprehensive and evenly distributed coverage of the input space. Therefore, adopting the LHS simulation requires fewer samples and a short calculation time while maintaining nearly the

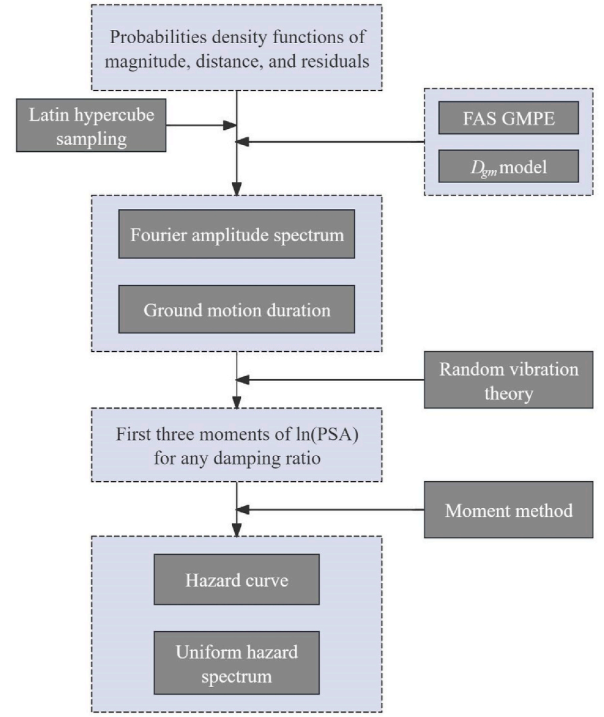


Fig. 4. Flowchart of the proposed framework for the computation of hazard curves of the PSA for various damping ratios.

same accuracy as that attained by the MC simulation.

Fig. 4 presents a flowchart of the proposed framework used for computing the seismic hazard curves of the PSA for various damping ratios. First, samples for each random variable and residual are generated based on the LHS according to their PDFs. Then, the FAS and ground-motion duration D_{gm} are estimated for each set of samples based on the selected FAS GMPE and D_{gm} model. Next, the PSA for various damping ratios is derived from the FAS and ground-motion duration D_{gm} according to Eq. (5), and subsequently, the first three statistical moments of $\ln(\text{PSA})$ can be obtained through statistical analysis. Finally, the CDFs of $\ln(\text{PSA})$ for different damping ratios are calculated using Eqs. (12)–(14). The exceedance probabilities and corresponding seismic hazard curves considering all earthquake sources are then derived using Eqs. (1) and (2).

Additionally, applying the proposed framework enables the consideration of epistemic uncertainties in the FAS GMPEs and duration models, similar to the traditional approach. A logic tree scheme employing multiple alternative GMPEs for the FAS and duration models with assigned weights can be used to address epistemic uncertainties. The calculation process simply involves repeating the procedure shown in Fig. 4 for each branch of the logic tree.

5. Numerical example

To demonstrate the efficiency and accuracy of the proposed framework, an example calculation was conducted in this section. This calculation example considers six hypothetical seismic zones, as shown in Fig. 5. The PDFs of the closest distance from the site to the surface projection of the rupture plane distance, R_{JB} , for the six seismic zones, are assumed to be lognormal according to a previous study [41]. For seismic zone A, the mean value of R_{JB} is 50 km; for seismic zone B, the mean value of R_{JB} is 100 km; for seismic zone C, the mean value of R_{JB} is 150 km; for seismic zone D, the mean value of R_{JB} is 289.50 km; for seismic zone E, the mean value of R_{JB} is 282.43 km; and for seismic zone F, the mean value of R_{JB} is 252.24 km. The standard deviations for seismic zones A, B, C, D, E, and F are 10 km, 20 km, 50 km, 61.42 km,

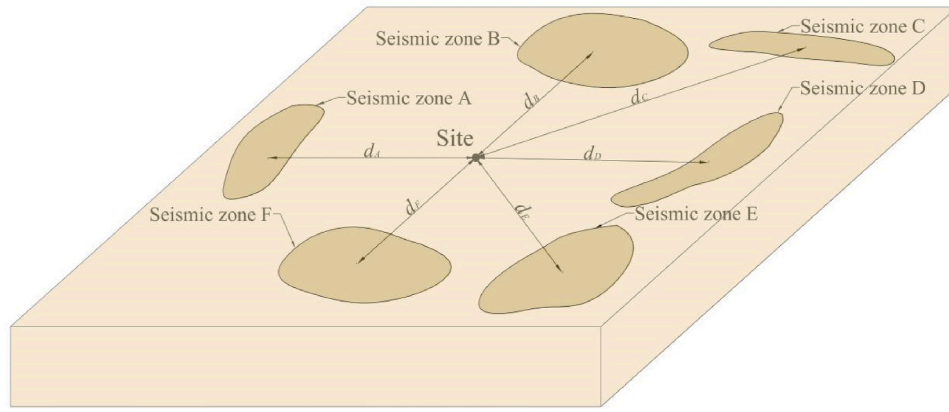


Fig. 5. Details of the seismic zones utilized for the numerical analysis.

24.22 km, and 40.11 km, respectively. The mean annual rates are 0.05 for seismic zone A, 0.06 for seismic zone B, 0.12 for seismic zone C, 0.04 for seismic zone D, 0.06 for seismic zone E, and 0.12 for seismic zone F. The widely used truncated exponential recurrence model is adopted as the PDF for magnitude [1,18,19,32,41], with the minimum threshold magnitude set to 6, and the maximum threshold magnitude set to 8. The statistical parameter θ is set to 2.6, based on previous studies [42,43], where θ was reported to range from 1.84 to 2.95. The time interval t is

set to 50 years. In addition, the time-averaged shear wave velocity in the upper 30m of the soil profile beneath the site, V_{s30} (m/s), is set to 760 m/s.

Many FAS GMPEs have been developed [16,20,21,23]. For the example calculation in this section, the FAS GMPE and ground-motion duration model developed by Bora et al. [16] were adopted. The FAS GMPE is expressed as

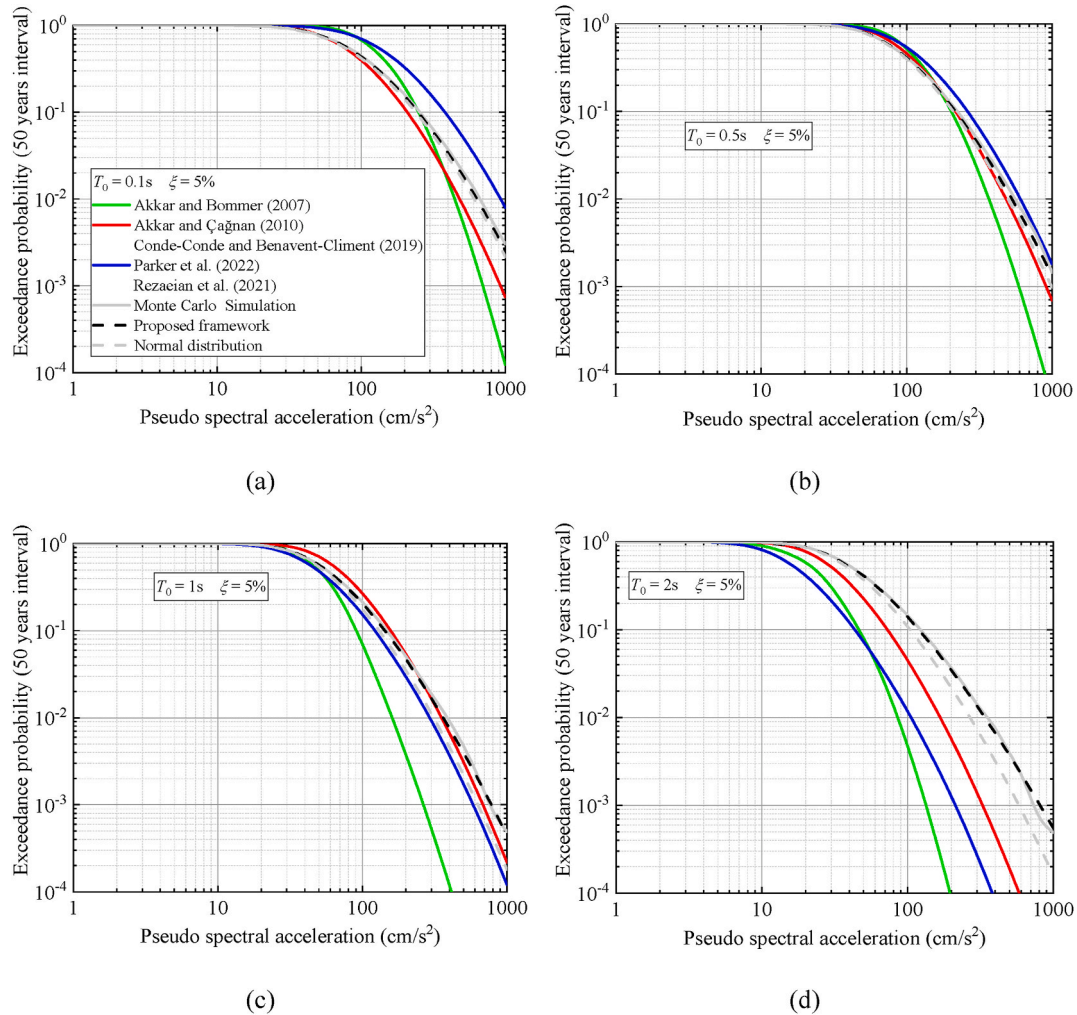


Fig. 6. Exceedance probabilities of the PSA at 50-year intervals for a 5 % damping ratio obtained using the proposed framework (3000 samples), MC simulation (100000 samples), and methods from previous studies for (a) $T_0 = 0.1s$, (b) $T_0 = 0.5s$, (c) $T_0 = 1s$, and (d) $T_0 = 2s$.

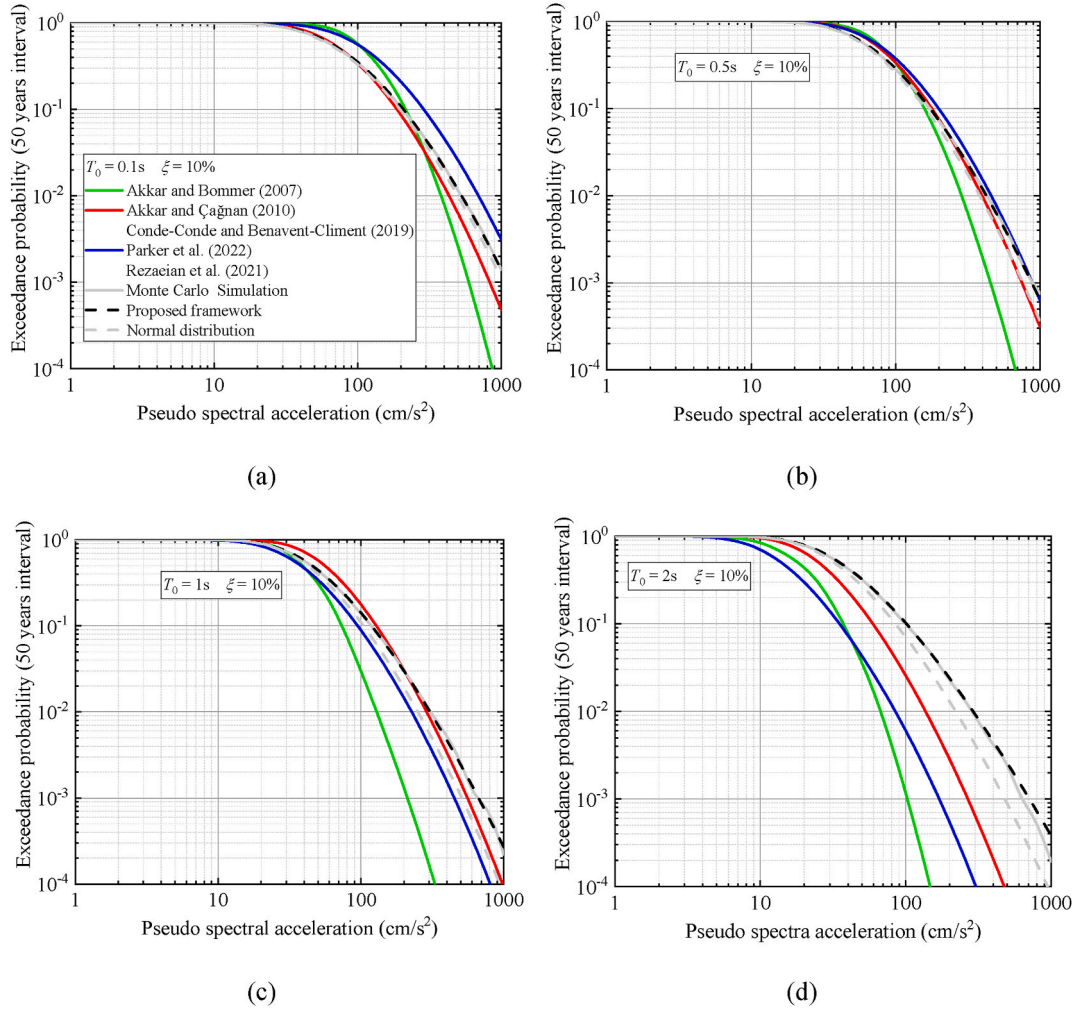


Fig. 7. Exceedance probabilities of the PSA at 50-year intervals for a 10 % damping ratio obtained using the proposed framework (3000 samples), MC simulation (100,000 samples), and methods from previous studies for (a) $T_0 = 0.1s$, (b) $T_0 = 0.5s$, (c) $T_0 = 1s$, and (d) $T_0 = 2s$.

$$\ln(Y(\omega)) = c_0 + c_1 M + c_2 M^2 + (c_3 + c_4 M) \ln \left(\sqrt{R_{JB}^2 + c_5^2} \right) - c_6 \sqrt{R_{JB}^2 + c_5^2} + c_7 \ln(Vs_{30}) + \eta + \varepsilon \quad (14)$$

In this equation, $Y(\omega)$ is the geometric mean of the FAS from the two horizontal components at a circular frequency ω . In addition, c_0 – c_7 are the regression coefficients for the FAS GMPE, η represents the between-event error, and ε represents the within-event error; they were assumed to be normally distributed with zero means and standard deviations τ and φ , respectively. The total standard deviation, σ , is calculated using the expression $\sigma = \sqrt{\tau^2 + \varphi^2}$. The values of the parameters c_0 – c_7 , τ , φ , and σ were given in Table 2 of Bora et al. [16].

The ground-motion duration D_{gm} model is expressed as,

$$\ln(D_{gm}) = c_0 + c_1 M + (c_2 + c_3 M) \ln \left(\sqrt{R_{JB}^2 + c_4^2} \right) + c_5 \ln(Vs_{30}) + \eta + \varepsilon \quad (15)$$

where D_{gm} is the geometric mean of the duration estimated from the two horizontal components and c_0 – c_5 are the regression coefficients for the D_{gm} model. The values of the standard deviations τ and φ of the between-event error η and within-event error ε , as well as the total standard deviation σ in Eq. (15) were all provided in Table 1 of Bora et al. [16].

It should be noted that when the proposed framework is applied in practice to a specific region for probabilistic analysis of the PSA across

multiple damping ratios, region-specific FAS GMPEs and duration models should be adopted to ensure their applicability. Neglecting regional seismological differences may lead to unrealistic ground motion estimations. The proposed framework is flexible and enables the use of any FAS GMPEs and duration models.

Then, the seismic hazard curves of the PSA for damping ratios of 5 %, 10 %, 20 %, 30 %, 40 %, and 50 % were calculated based on the proposed framework. A total of 3000 samples were generated for each random variable and residual based on the LHS. These results were then compared with those obtained from MC simulation using 100000 samples for each random variable. Representative comparisons are depicted in Figs. 6–9. Fig. 6 presents seismic hazard curves of the PSA for a damping ratio of 5 %, Fig. 7 presents seismic hazard curves of the PSA for a damping ratio of 10 %, Fig. 8 presents seismic hazard curves of the PSA for a damping ratio of 30 %, and Fig. 9 presents seismic hazard curves of the PSA for a damping ratio of 50 %.

First, it can be observed that the proposed framework can simultaneously provide seismic hazard curves for various damping ratios. In addition, the results of the proposed framework agree very well with those of the MC simulation. Moreover, the proposed framework requires only 3/100 of the calculation time of the MC simulation. The MC simulations took approximately 4 h to calculate the results of each figure for each damping ratio, whereas the proposed framework required less than 3 min.

Seismic hazard curves from the proposed framework are compared with those from the traditional PSHA framework in Figs. 6–9. The

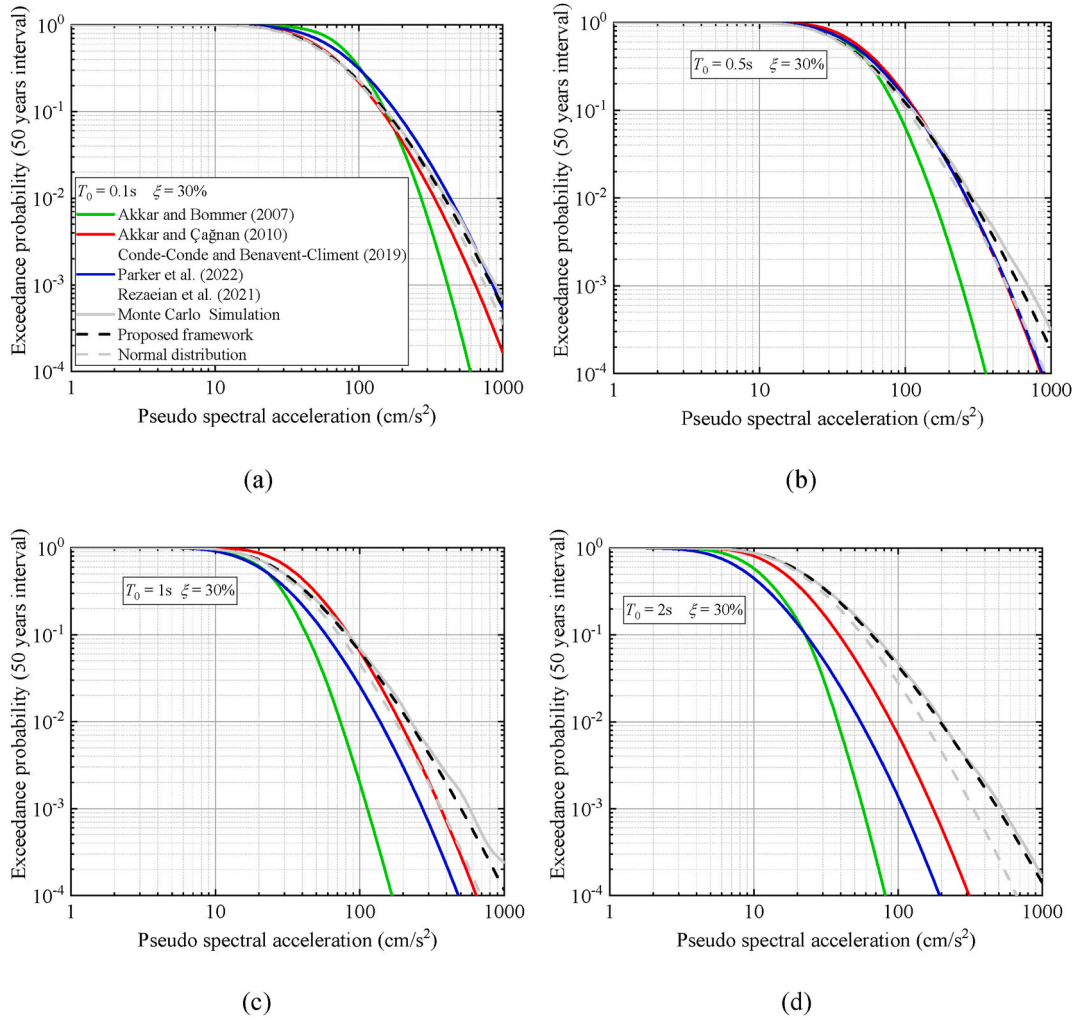


Fig. 8. Exceedance probabilities of the PSA at 50-year intervals for a 30 % damping ratio obtained using the proposed framework (3000 samples), MC simulation (100000 samples), and methods from previous studies for (a) $T_0 = 0.1s$, (b) $T_0 = 0.5s$, (c) $T_0 = 1s$, and (d) $T_0 = 2s$.

traditional PSHA framework adopts two pairs of 5 %-damped GMPEs in conjunction with DMF models, as well as PSA GMPEs at various damping ratios from a previous study, to estimate the PSA for different damping levels. Because Bora et al. [16] found that the median PSA values predicted from the FAS GMPE used in this study closely match those predicted from the PSA GMPE of Akkar and Çağnan [44], the GMPE proposed by Akkar and Çağnan [44] is adopted for comparison. This 5 %-damped GMPE, developed using European ground motions, is adjusted to other damping levels using the DMF proposed by Conde-Conde and Benavent-Climent [45], which is also based on European data. Although the standard deviation of the PSA is known to vary with the damping ratio, most DMF models, including that of Conde-Conde and Benavent-Climent [45], focus solely on the median values and neglect the standard deviation. Therefore, the standard deviation of the GMPE proposed by Akkar and Çağnan [44] is assumed to remain constant across all damping ratios in this study. Additionally, a recent global PSA GMPE proposed by Parker et al. [46], in conjunction with a global DMF model developed by Rezaeian et al. [15], is also adopted for comparison. Both models were developed based on the database of Next Generation Attenuation for the subduction earthquakes project. The standard deviation models of the PSA and DMF proposed by Parker et al. [46] and Rezaeian et al. [15], respectively, enable the determination of the PSA standard deviations for different damping ratios. Moreover, Akkar and Bommer [14] developed GMPEs for the PSA for multiple damping levels (2 %, 5 %, 10 %, 20 %, and 30 %) based on

seismic records from Europe and the Middle East, which are also used to generate seismic hazard curves. The standard deviations of Akkar and Bommer [14] were developed directly as a function of the damping ratio. Both the models proposed by Akkar and Çağnan [44] and Akkar and Bommer [14] include a faulting style term, and the strike-slip mechanism is used for comparison. Rezaeian et al. [15] and Parker et al. [46] developed models for both interface and intra-slab subduction earthquakes, in this study, the models for interface subduction earthquakes are adopted for comparison.

It can be observed from Figs. 6–9 that the seismic hazard curves from the proposed framework are very similar to those from the models of Akkar and Çağnan [44] and Conde-Conde and Benavent-Climent [45], except for $T_0 = 2s$. The similarity is primarily because the median PSA values predicted using the FAS GMPE applied in this study closely match those derived from the PSA GMPE proposed by Akkar and Çağnan [44], as noted by Bora et al. [16]. The similarity also provides some evidence for the validity of the proposed framework. The differences between the two frameworks, particularly for $T_0 = 2s$, may be attributed to the differences in the standard deviation and the methods used to handle changes in the median values and standard deviation with respect to the damping ratio. The proposed framework accounts for the effects of the damping ratio on the PSA median values and standard deviation using RVT (Eq. (5)), whereas the traditional PSHA framework incorporates these effects using additional DMF models.

In addition, although the FAS GMPE adopted in this study and the

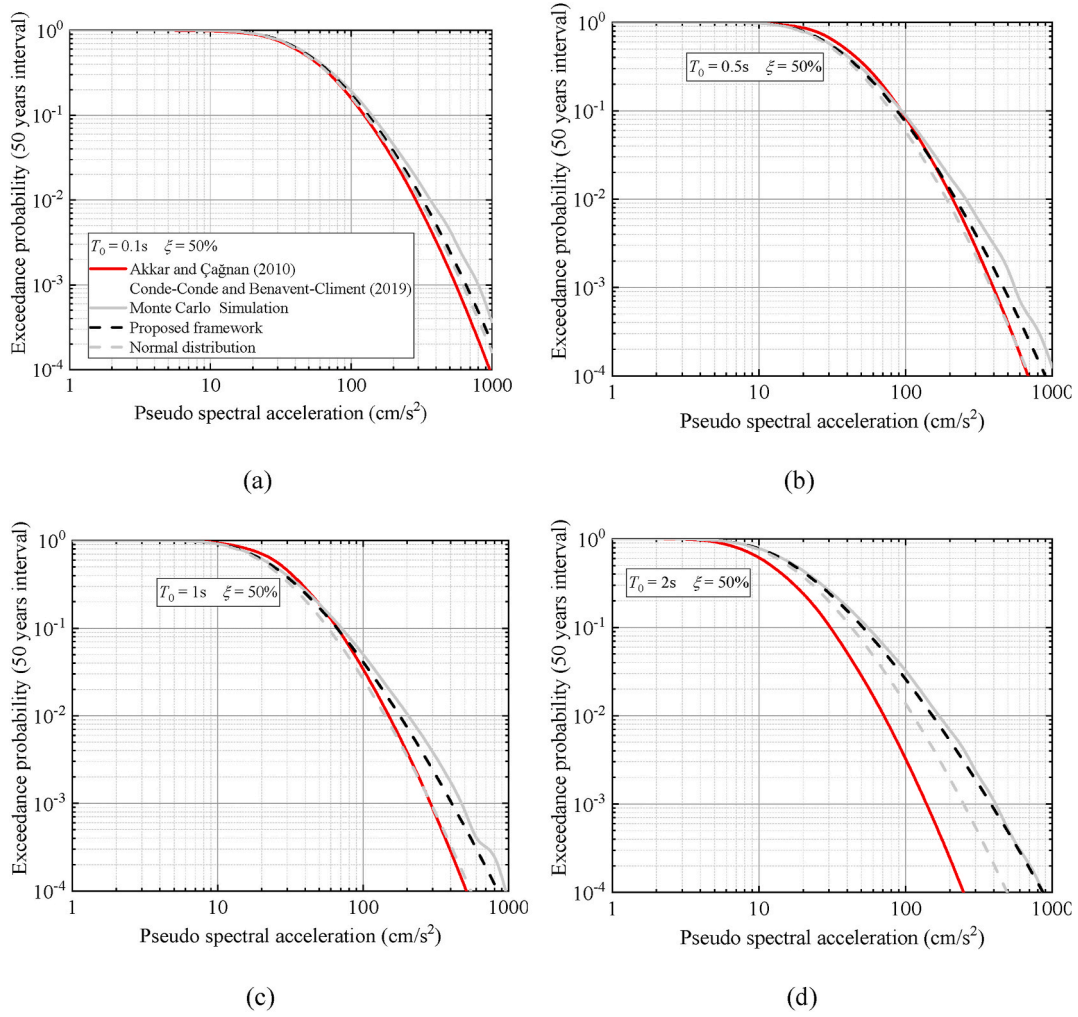


Fig. 9. Exceedance probabilities of the PSA at 50-year intervals for a 50 % damping ratio obtained using the proposed framework (3000 samples), MC simulation (100000 samples), and methods from previous studies for (a) $T_0 = 0.1s$, (b) $T_0 = 0.5s$, (c) $T_0 = 1s$, and (d) $T_0 = 2s$.

models of Parker et al. [46] and Rezaeian et al. [15] were developed using different databases, their results are generally comparable, except for $T_0 = 2s$. However, the differences between the results from the proposed framework and those obtained using the model of Akkar and Bommer [14] are significantly more pronounced. This discrepancy is primarily because Akkar and Bommer [14] adopted magnitude-dependent standard deviations that were later deemed unreasonable, as noted by Akkar and Bommer [47]. In general, compared with the traditional PSHA framework, the proposed framework accounts for the effects of the damping ratio on the PSA median values and standard deviation using RVT (Eq. (5)), eliminating the need to construct multiple GMPEs for various damping ratios or develop DMF and standard deviation models.

Furthermore, to highlight the advantages of using the three-parameter distribution over the traditional normal distribution, seismic hazard curves from the proposed framework—where the three-parameter distribution is replaced with the normal distribution—are also shown in Figs. 6–9. It can be observed that as the period increases, the results obtained using the three-parameter distribution align more closely with those of the MC simulation than those obtained using the normal distribution. This is because the three-parameter distribution provides a better fit for the statistical data, particularly over long periods where skewness is present. Fig. 10 shows an example comparison of the three-parameter and normal distributions when fitting the distribution of $\ln(\text{PSA})$ ($T_0 = 10s$) for seismic zone C.

Moreover, uniform hazard spectra for various damping ratios are computed using the proposed framework and compared with those obtained using the traditional approach by employing DMF formulations. Two DMF formulations from Eurocode 8 [48] and ASCE-07 [49] are used for adjusting the 5 %-damped uniform hazard spectra, and the results are shown in Figs. 11 and 12, respectively. Two exceedance probabilities, namely, 2 % and 10 % in 50 years, were considered in the calculation. It is observed that the results obtained using the DMF formulations can deviate significantly from those derived using the proposed framework, with the deviation increasing as the damping ratio increases. In addition, the DMF, calculated as the ratio of the uniform hazard spectra for various damping ratios to that for a 5 % damping ratio, is compared with those obtained from the previous DMF formulas, as shown in Fig. 13. The results indicate that the DMF derived from the proposed framework depends not only on the damping ratio but also on the period and, to a lesser extent, on the exceedance probability. The DMF values from Eurocode 8 [48] and ASCE-07 [49] can deviate significantly from those obtained using the proposed framework, particularly over short periods. Although the results from Conde-Conde and Benavent-Climent [45] agree more closely with the proposed framework, noticeable deviations over short periods can still be observed. These deviations may have arisen because the development of the DMF formulations did not consider the recurrence periods of the response spectra, resulting in the adjusted spectra having a different recurrence period than the 5 %-damped spectra. Alternatively, this may

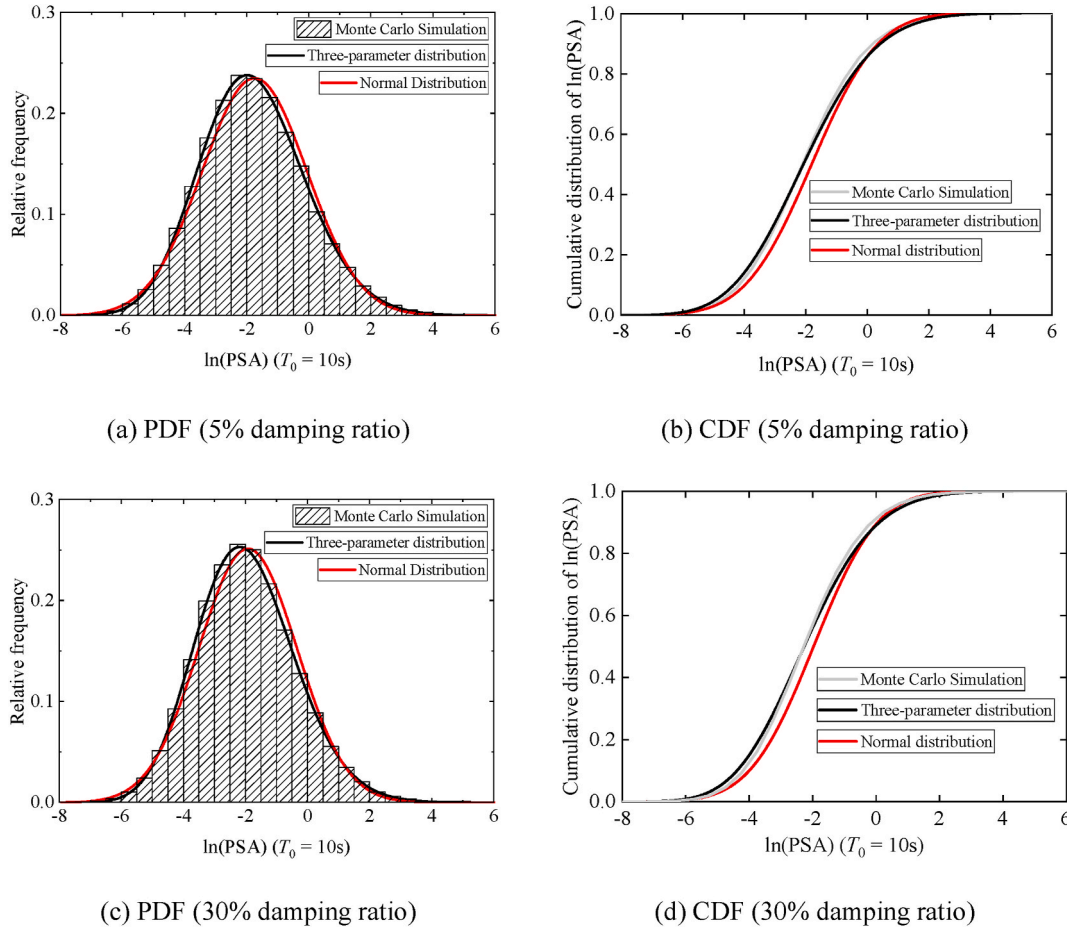


Fig. 10. Comparisons of the three-parameter and normal distributions when fitting the distribution of $\ln(\text{PSA})$ ($T_0 = 10$ s) for seismic zone C.

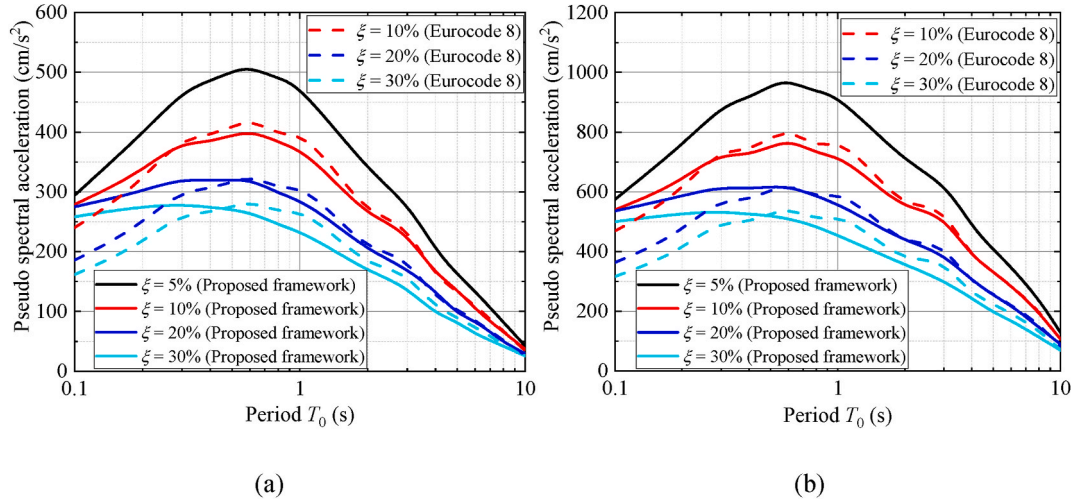


Fig. 11. Comparison of uniform hazard spectra for different damping ratios obtained using the proposed framework and the traditional approach that adopts the DMF formulation in Eurocode 8 (2004), for the exceedance probabilities of (a) 10 % in 50 years and (b) 2 % in 50 years.

be because the earthquakes considered for deriving these DMF formulations differ from those considered in PSHA. Regardless of the reason, the proposed framework demonstrates clear advantages over traditional approaches in estimating the PSA for distinct recurrence periods at any desired damping ratio.

6. Conclusions

This study developed a framework for conducting a probabilistic analysis of the pseudo spectral acceleration (PSA) for various damping ratios, providing a means to directly obtain the PSA corresponding to distinct recurrence periods for any desired damping ratio. The framework estimates the site-specific PSA from an earthquake source using a

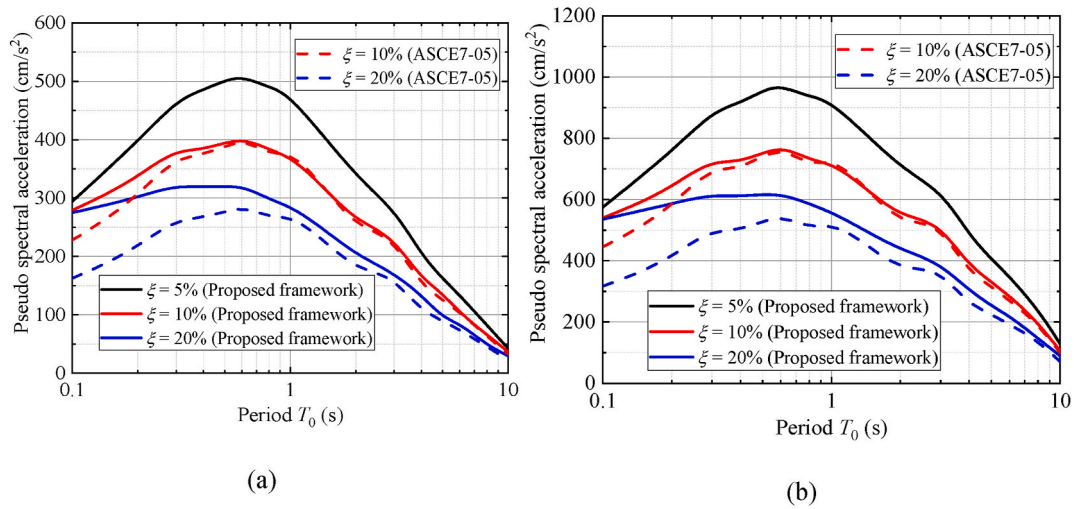


Fig. 12. Comparison of uniform hazard spectra for different damping ratios obtained using the proposed framework and the traditional approach that adopts the DMF formulation in ASCE7-05 (2006), for the exceedance probabilities of (a) 10 % in 50 years and (b) 2 % in 50 years.

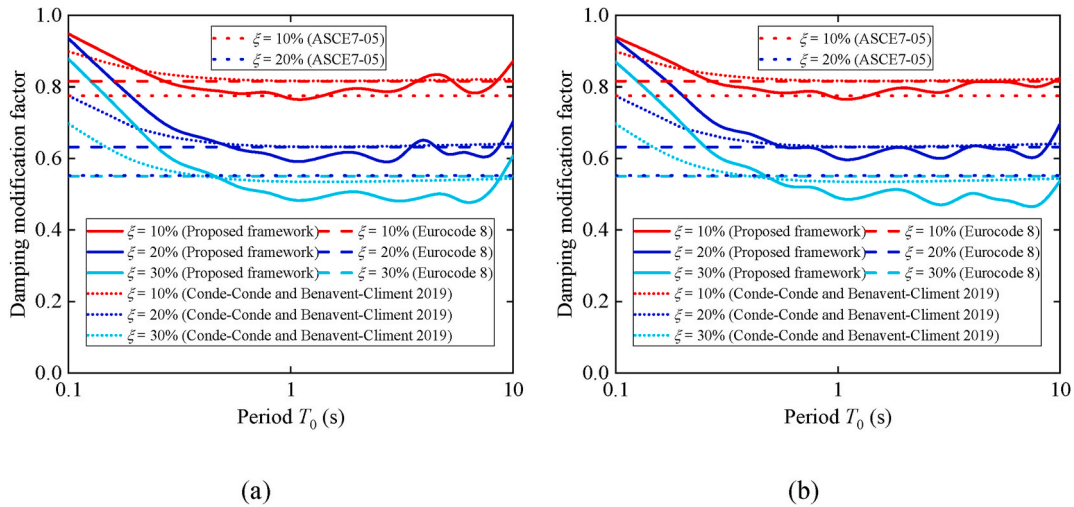


Fig. 13. Comparison of damping modification factors obtained using the proposed framework and the previous formulas for the exceedance probabilities of (a) 10 % in 50 years and (b) 2 % in 50 years.

ground-motion prediction equation (GMPE) for the Fourier amplitude spectrum (FAS) combined with a ground-motion duration model. This framework is preferable to the traditional one because the FAS is more closely related to the physics of wave propagation, and its scaling within GMPEs is easier to constrain using seismological theory. Additionally, the moment method, in combination with Latin hypercube sampling, is employed to calculate the exceedance probabilities of the PSA for any damping ratio, enabling the generation of corresponding seismic hazard curves. The primary conclusions of this study are as follows.

- (1) The accuracy of the approach used for estimating the PSA for various damping ratios from the FAS and the duration of ground motion based on random vibration theory was confirmed by comparing the results with those from a time-series analysis.
- (2) An example calculation was conducted to validate the proposed framework by considering six seismic zones. The proposed framework is highly efficient, requiring only 3/100 of the calculation time of the Monte Carlo (MC) simulation, however, it achieves nearly the same level of accuracy as the MC simulation.
- (3) The results of the proposed framework were compared with those of the traditional PSHA framework. The proposed framework

accounts for the effects of the damping ratio on the PSA median values and standard deviation by utilizing random vibration theory, eliminating the need to construct multiple GMPEs for various damping ratios or to construct DMF and standard deviation models.

- (4) Uniform hazard spectra for various damping ratios are computed by applying the proposed framework and compared with those obtained from the traditional approach employing DMF formulations. The results from the DMF formulations can deviate significantly from those obtained using the proposed framework, with the deviation increasing as the damping ratio increases.

CRediT authorship contribution statement

Haizhong Zhang: Writing – review & editing, Writing – original draft, Software, Methodology, Data curation, Conceptualization. **Rui Zhang:** Methodology, Investigation, Data curation. **Yan-Gang Zhao:** Writing – review & editing, Visualization, Supervision. **Hongjun Si:** Writing – review & editing, Visualization, Validation, Supervision. **Haixiu Zhang:** Writing – review & editing, Visualization, Data curation.

Funding

The research leading to these results received fundings from the Japan Society for the Promotion of Science (JSPS) KAKENHI (Grant No. 24K17336) as well as the National Key R&D Program of China (2023YFC3805100, 2023YFC3805101).

Declaration of competing interest

The authors declare that they have no known competing financial interests or personal relationships that could have appeared to influence the work reported in this paper.

Acknowledgments

This work was supported by the Japan Society for the Promotion of Science (JSPS) KAKENHI (Grant No. 24K17336) as well as the National Key R&D Program of China (2023YFC3805100, 2023YFC3805101), the authors are grateful for the financial supports.

Data availability

The Fourier amplitude spectra and time series used in the analysis were created using the Stochastic-Method SIMULATION (SMSIM) programs obtained from http://daveboore.com/software_online.html (last accessed on March 5, 2024).

References

- Tselentis GA, Danciu L, Sokos E. Probabilistic seismic hazard assessment in Greece - Part 2: acceleration response spectra and elastic input energy spectra. *Nat Hazards Earth Syst Sci* 2010;10(1):41–9.
- Pradhan PM, Timsalsina SP, Bhatt MR. Report on construction of design response spectrum for Nepal: a probabilistic approach. Bhaktapur, Nepal: University Grants Commission (UGC-Nepal) Research division Sanothimi; 2020.
- Rezaeian S, Powers PM, Shumway AM, Petersen MD, Luco N, Frankel AD, Moschetti MP, Thompson EM, McNamara DE. The 2018 update of the US National Seismic Hazard Model: ground motion models in the central and eastern US. *Earthq Spectra* 2021;37(1_suppl):1354–90.
- Building Seismic Safety Council (BSSC). NEHRP recommended seismic provisions for new buildings and other structures. 2015 edition. Federal Emergency Management Agency Report P-1050-1; 2015.
- Building Seismic Safety Council (BSSC). NEHRP recommended seismic provisions for new buildings and other structures. 2020 edition. Federal Emergency Management Agency Report P-2082-1; 2020.
- Constantinou MC, Soong TT, Dargush GF. Passive energy dissipation systems for structural design and retrofit. New York: Monograph series, MCEER, Buffalo; 1998.
- Naem F, Kelly JM. Design of seismic isolated structures. From theory to practice. New York: John Wiley and Sons; 1999.
- Hatzigeorgiou GD. Damping modification factors for SDOF systems subjected to near-fault, far-fault and artificial earthquakes. *Earthq Eng Struct Dynam* 2010;39(11):1239–58.
- Lin YY, Chang KC. Effects of site classes on damping reduction factors. *J Struct Eng* 2004;130(11):1667–75.
- Zhang HZ, Zhao YG. Damping modification factor based on random vibration theory using a source-based ground-motion model. *Soil Dynam Earthq Eng* 2020;136:106225.
- Zhang HZ, Zhao YG. Damping modification factor of acceleration response spectrum considering seismological effects. *J Earthq Eng* 2022;26(16):8359–82.
- Zhang HZ, Deng J, Zhao YG. Damping modification factor of pseudo-acceleration spectrum considering influences of magnitude, distance and site conditions. *Earthquakes and Structures* 2023;25(3):325–42.
- Surana M, Singh Y, Lang DH. Damping modification factors observed from the Indian strong-motion database. *J Earthq Eng* 2019;25(13):2758–73.
- Akkar S, Bommer JJ. Prediction of elastic displacement response spectra in Europe and the Middle East. *Earthq Eng Struct Dynam* 2007;36:1275–301.
- Rezaeian S, Atik LA, Kuehn NM, Abrahamson M, Bozorgnia Y, Mazzoni S, Withers K, Campbell K. Spectral damping scaling factors for horizontal components of ground motions from subduction earthquakes using NGA-Subduction data. *Earthq Spectra* 2021;37(4):2453–92.
- Bora SS, Scherbaum F, Kuehn N, Stafford P. Fourier spectral- and duration models for the generation of response spectra adjustable to different source-, propagation-, and site conditions. *Bull Earthq Eng* 2014;12:467–93.
- Bayless J, Abrahamson NA. Summary of the BA18 ground-motion model for Fourier amplitude spectra for crustal earthquakes in California. *Bull Earthq Eng* 2019;109(5):2088–105.
- Zhao YG, Zhang R, Zhang HZ. Probabilistic prediction of ground-motion intensity for regions lacking strong ground-motion records. *Soil Dynam Earthq Eng* 2023;165:107706.
- Zhang R, Zhao YG, Zhang HZ. An efficient method for probability prediction of peak ground acceleration using Fourier amplitude spectral model. *J Earthq Eng* 2024;28(6):1495–511.
- Lavrentiadis G, Abrahamson NA, Kuehn NM. A non-ergodic effective amplitude ground-motion model for California. *Bull Earthq Eng* 2023;21:5233–64.
- Sung CH, Abrahamson NA, Kuehn NM, Traversa P, Zentner I. A non-ergodic ground-motion model of Fourier amplitude spectra for France. *Bull Earthq Eng* 2023;21:5293–317.
- Boore DM. Simulation of ground motion using the stochastic method. *Pure Appl Geophys* 2003;160(3):635–76.
- Meenakshi Y, Sreenath V, Stg R. Ground motion models for Fourier amplitude spectra and response spectra using machine learning techniques. *Earthq Eng Struct Dynam* 2024;53(2):756–83.
- Cartwright DE, Longuet-Higgins MS. The statistical distribution of the maxima of a random function. *Proceedings of the Royal Society A Mathematical, Physical and Engineering Sciences* 1956;237(1209):212–32.
- Davenport AG. Note on the distribution of the largest value of a random function with application to gust loading. *Proc Inst Civ Eng* 1964;28(2):187–96.
- Vanmarcke EH. On the distribution of the first-passage time for normal stationary random processes. *J Appl Mech* 1975;42(1):215–20.
- Wang XY, Rathje EM. Influence of peak factors on site amplification from random vibration theory based site-response analysis. *Bull Seismol Soc Am* 2016;106(4):1733–46.
- Boore DM, Joyner WB. A note on the use of random vibration theory to predict peak amplitudes of transient signals. *Bull Seismol Soc Am* 1984;74(5):2035–9.
- Liu L, Pezeshk S. An improvement on the estimation of pseudoresponse spectral velocity using RVT method. *Bull Seismol Soc Am* 1999;89(5):1384–9.
- Boore DM, Thompson EM. Revisions to some parameters used in stochastic-method simulations of ground motion. *Bull Seismol Soc Am* 2015;105(2A):1029–41.
- Zhang HZ, Zhao YG. Effects of magnitude and distance on spectral and pseudo spectral acceleration proximities for high damping ratio. *Bull Earthq Eng* 2022;20:3715–37.
- Zhang HZ, Zhang R, Zhao YG. Novel approach for energy-spectrum-based probabilistic seismic hazard analysis in regions with limited strong earthquake data. *Earthq Spectra* 2024. <https://doi.org/10.1177/87552930241263621>.
- Boore DM. SMSIM - fortran programs for simulating ground motions from earthquakes: version 2.3 – a revision of OFR 96-80-A. Tech. Rep., Reston, VA: United States Geological Survey; 2005.
- Boore DM. Stochastic simulation of high-frequency ground motions based on seismological models of the radiated spectra. *Bull Seismol Soc Am* 1983;73(6A):1865–94.
- Nigam N, Jennings P. Calculation of response spectra from strong-motion earthquake records. *Bull Seismol Soc Am* 1969;59(2):909–22.
- Baker JW. An introduction to probabilistic seismic hazard analysis (PSHA). 2008. p. 24–36. version 1.3. [https://www.jackwbaker.com/Publications/Baker_\(2008\)_Intro_to_PSHA_v1_3.pdf](https://www.jackwbaker.com/Publications/Baker_(2008)_Intro_to_PSHA_v1_3.pdf). [Accessed 26 September 2024].
- Zhao YG, Ono T. Moments methods for structural reliability. *Struct Saf* 2001;23(1):47–75.
- Zhao YG, Ono T, Idota H, Hirano T. A three-parameter distribution used for structural reliability evaluation. *Journal of Structural and Construction Engineering (Transactions of AIJ)* 2001;66(546):31–8.
- Zhao YG, Lu ZH. Structural reliability: approaches from perspectives of statistical moments. America: Hoboken: Wiley; 2021.
- McKay MD, Beckman RJ, Conover WJ. A comparison of three methods for selecting values of input variables in the analysis of output from a computer Code. *Technometrics* 1979;21(2):239–45.
- Alamilla JL, Rodriguez JA, Vei R. Unification of different approaches to probabilistic seismic hazard analysis. *Bull Seismol Soc Am* 2020;110(6):2816–27.
- Abdulnaby W, Onur T, Gök R, et al. Probabilistic seismic hazard assessment for Iraq. *J Seismol* 2020;24:595–611.
- Villani M, Lubkowski Z, Free M, et al. A probabilistic seismic hazard assessment for Wylfa Newydd, a new nuclear site in the United Kingdom. *Bull Earthq Eng* 2020;18:4061–89.
- Akkar S, Çağnan C. A local ground-motion predictive model for Turkey, and its comparison with other regional and global ground-motion models. *Bull Seismol Soc Am* 2010;100(6):2978–95.
- Conde-Conde J, Benavent-Climent A. Construction of elastic spectra for high damping. *Eng Struct* 2019;191:343–57.
- Parker GA, Stewart JP, Boore DM, Atkinson GM, Hassani B. NGA-subduction global ground motion models with regional adjustment factors. *Earthq Spectra* 2022;38(1):456–93.
- Akkar S, Bommer JJ. Empirical equations for the prediction of PGA, PGV, and spectral accelerations in Europe, the mediterranean region, and the Middle East. *Seismol Res Lett* 2010;81(2):195–206.
- Eurocode 8. Design of structures for earthquake resistance, Part 1: general rules, seismic actions and rules for buildings, EN 2004-1-1. Brussels: CEN; 2004.
- ASCE 7-05. Minimum design loads for buildings and other structures. Reston, VA, USA: American Society of Civil Engineers; 2006.